Ab initio study of nitrogen and boron substitutional impurities in single-wall SiC nanotubes

A. Gali
Department of Atomic Physics, Budapest University of Technology and Economics, Budafoki út 8, H-1111, Budapest, Hungary
(Received 4 February 2006; revised manuscript received 23 March 2006; published 15 June 2006)

Silicon carbide nanotubes have a great potential for application in chemical sensors in harsh environment or in biological sensors. It is of interest to explore the electronic properties of these nanotubes, and how those are modified in the presence of impurities. It is well known that nitrogen and boron atoms are common contaminations in bulk silicon carbide (SiC). Nitrogen preferentially substitutes the carbon site making *n*-type conductivity in bulk SiC. Boron substitutes both carbon and silicon sites forming a deep and a shallow acceptor in bulk SiC, respectively. In this paper we have studied these defects in armchair and zig-zag SiC nanotubes by *ab initio* supercell calculations. We found that nitrogen forms relatively shallow or deep donor state depending on the width of the band gap of the SiC nanotube. Boron is a relatively deep or shallow acceptor at carbon and silicon sites, respectively, like in bulk SiC polytypes. The site preference of boron depends on the stoichiometry of the SiC nanotubes. We have found no significant difference in the properties of boron substitutional defect between armchair and zig-zag nanotubes.

DOI: 10.1103/PhysRevB.73.245415 PACS number(s): 61.72.Bb, 71.15.Mb, 71.55.Ht, 61.72.Ji

I. INTRODUCTION

Bulk silicon carbide (SiC) is a wide band gap semiconductor with a great potential for application in high-power high-temperature electronics. Porous SiC was found to be a biocompatible material and already successfully used in bone implants. Based on the spirit of the tubular forms of carbon atoms,[1] called carbon nanotubes, tubular forms of silicon carbide have been searched and investigated both in experiments and by theory. Forms of nanocables, nanorods and nanowires from SiC were already found,[2,3] while recently various structures of SiC nanotubes have been reported.[4] These SiC nanotubes have been synthesized via the reaction of SiO with multiwalled carbon nanotubes at different temperatures. The produced multiwalled SiC nanotubes have interlayer space ranging from 3.8 Å to 4.5 Å, significantly larger than 3.4 Å found in carbon nanotubes.[4] The transformation of SiC nanotubes to the 3*C*-SiC structure have been also observed under an electron beam annealing at the energy of 200 keV,[4] which indicates that the SiC nanotubes are metastable forms with respect to the bulk (3*C*)SiC. While only multiwalled SiC nanotubes were produced the large distance between the walls may suggest that the walls are independent of others and can be considered to be single wall nanotubes. In any case it is of interest to explore the properties of single wall SiC nanotubes whether it is worth making an effort to produce them. The structure and stability of SiC single wall nanotubes have been investigated by *ab initio* theory in detail.[5–7] It was found that the SiC nanotubes with alternating Si-C bonds are energetically preferred over the forms which contain C-C or Si-Si bonds.[6] Single wall SiC nanotubes are semiconductors independent from the helicity unlike the case of carbon nanotubes.[5–7] It is interesting to note that the bulk SiC polytypes are indirect semiconductors while the zig-zag SiC single wall nanotubes are direct semiconductors.[5] *Ab initio* supercell calculations have shown[8] that hydrogenation of single wall SiC nanotubes can strongly modify their electronic structure. It was also found that SiH_3 or CH_3 molecules can bind to single wall SiC nanotubes forming acceptor or donor levels depending on the adsorption sites.[9]

It is well known that nitrogen and boron is a common impurity in crystalline SiC. Nitrogen preferentially substitutes the carbon site (N_C) and is a relatively shallow donor. Theoretical calculations showed that the formation energy of nitrogen substitutional at the silicon site (N_{Si}) is more than 5 eV higher than that of N_C.[10–12] Boron substitutes both carbon and silicon sites in bulk SiC depending on the forming conditions according to the calculations.[13–15] Theory[13,16,17] and experiment[18,19] agreed that B_{Si} forms the shallow boron acceptor. Calculations showed that B_C is a deeper acceptor[13,16] than B_{Si} and is most probably identical to the *D* deep level transient spectroscopy center,[14,20,21] i.e., the deep boron acceptor. In chemical vapor deposited (CVD) SiC epitaxial layers it has been problematic to avoid the nitrogen incorporation making the samples *n*-type. Semi-insulating SiC substrates could be produced just recently by introducing native compensating defects.[22,23] Boron is also a common impurity in CVD SiC layers. Larkin and co-workers have been able to produce SiC nanobamboos by using the partly CVD technique.[24] It may happen that nitrogen and boron impurities can enter SiC nanotubes like in crystalline SiC layers modifying their electronic properties. It is desirable to study the effect of these impurities in SiC nanotubes. In this paper we have investigated the structure and electronic properties of substitutional nitrogen and boron impurities in armchair and zig-zag single wall SiC nanotubes by means of *ab initio* supercell calculations.

II. METHODOLOGY

Following the work of Zhao and co-workers[7] we have investigated the impurities in a typical armchair and in a typical zig-zag single wall SiC nanotube. Those are the (6,6) and (8,0) SiC nanotubes, respectively. The structure and electronic properties were determined by density functional theory (DFT) calculations within the local spin density approximation (LSDA).[25] We used the SIESTA code[26] package

 ©2006 The American Physical Society

to accomplish this task. We applied the Ceperley-Alder exchange-correlation functional[27] as parameterized by Perdew and Zunger.[28] Troullier-Martins pseudopotentials were used to take the effect of core electrons into account.[29] The given core radii in the construction of the pseudopotentials were 1.89, 1.25, 1.24, and 1.78 bohr for Si, C, N, and B atoms, respectively. We applied a double-ζ plus polarization function basis set which is given by the code.[26] We used the 0.02 Ry energy shift to compress the basis set and to accelerate the calculations (see the SIESTA package for detailed description).[26] The charge density was projected onto a real-space grid with an equivalent cutoff of 90 Ry. These parameters provided results equivalent to those of well-converged plane wave calculations for bulk SiC.[30]

The SIESTA package applies the supercell approach in three dimensions. We have used approximately 10 Å vacuum in the lateral directions to avoid artificial tube-tube interaction. This should be sufficient distance since the basis functions do not overlap. First, the lattice vector and the coordinates of atoms were optimized in (6,6) and (8,0) single wall SiC nanotubes, with 24 and 32 basis atoms in the primitive cells, respectively. The stopping criteria in the optimization process of the conjugate gradient algorithm were 10^{-6}eV/Å^{3}for each component of the stress tensor and 0.02 eV/Å for the atomic forces. We used 8 Monkhorst-Pack (MP) special k points along the tube axis during this process.[31] The convergence tests on the aforementioned parameters have been carried out and are reported in the next section. We used a 96-atom (6,6) and a 128-atom (8,0) supercell in order to investigate the defects. In this case 4 MP k points along the tube axis were used. All the atoms in these defective supercells were allowed to relax until the atomic forces were below 0.02 eV/Å. We used spin-polarized calculations for systems with odd number of electrons.

DFT-LSDA calculations underestimate the band gaps of semiconductors. It has been recently shown that hybrid functionals can reproduce the band gaps of semiconductors and insulators consistently well.[32,33] We recalculated the band structure of the perfect and defective supercells optimized by the SIESTA code within the same k point set by using a hybrid functional in order to check the DFT-LSDA error.[34] Following the suggestion of Becke,[35] a one-parameter hybrid functional was used in this work. The CRYSTAL2003 code was used to accomplish this task.[36] Like in SIESTA, the Ceperley-Alder exchange-correlation functional in the Perdew-Zunger parameterization was used, with the exchange part mixed with exact exchange following the equation

$$E_{XC} = E_{XC}^{LSDA} + \lambda(E_X^{exact} - E_X^{LSDA}). \quad (1)$$

We used $\lambda=0.20$ in this study. Norm-conserving Durand-Barthelat[37] pseudopotentials and a $21G^*$ valence basis[38] optimized for these pseudopotentials were applied for the atoms. We have shown earlier that this methodology reproduces the band gap of different polytypes very well: [30] 2.4 eV for 3C-SiC and 3.3 eV for 4H-SiC. The calculated occupied defect levels fell practically at the same position with this method as with an approximate LDA+GW method[39] in bulk SiC.[15] The localized empty defect levels are, however, usually placed much higher in energy by BLYP than by LDA+GW method, so the position of the BLYP empty defect levels cannot be directly compared to vertical ionization energies.

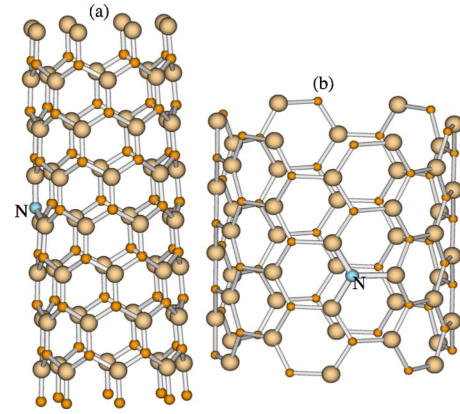

FIG. 1. (Color online) The optimized geometry of N_C in (a) (8,0), (b) (6,6) single wall SiC nanotubes. The large balls are the silicon atoms, the smaller balls are the carbon atoms. The nitrogen atom is labeled.

III. RESULTS

A. Perfect zig-zag (8,0) and armchair (6,6) single wall SiC nanotubes

We optimized first the zig-zag (8,0) single wall SiC nanotube. The calculated Si-C bond length is about 1.78 Å in accordance with Ref. 5 which used the same LSDA functional and well-converged cutoff of 40 Ry of the plane wave basis set. This result is also identical to that obtained in Ref. 9 by using practically the same method and parameters as expected. Similar to boron nitride nanotubes,[40] the more electronegative atoms (C atoms) move radially outward and the more electropositive (Si atoms) move inward, resulting in a rippled surface. The calculated average diameter is about 7.9 Å, while the optimized lattice constant is about 5.32 Å. The calculated band structure along Γ-X basically agrees with earlier works using similar methodology;[7,8] we obtained a direct semiconductor, where the minimum of the conduction band edge (CBM) and the maximum of the valence band edge (VBM) are at the Γ point. However, there is a slight difference between those studies and this work; the calculated LDA band gap is about 1.21 eV while only 0.9 eV reported in the earlier studies.[7,8] Zhao and co-workers[7] used a generalized gradient corrected approximation (GGA) in the calculations which may result in a difference, however, the GGA band gaps are usually larger than the LDA band gaps. Therefore, we have carried out careful tests on the used parameters in the calculations. Raising the number of MP k points to 32 along the tube axis results in less than 0.01 eV increase in the width of the band gap. We increased the cutoff of the charge density to 180 Ry from 90 Ry, which resulted in less than 0.02 eV increase in the width of the band gap. We also tried to decrease the energy shift value (to use less compressed basis functions) from 0.02 Ry to 0.01 Ry. Again, this results in less than 0.03 eV increase in the width

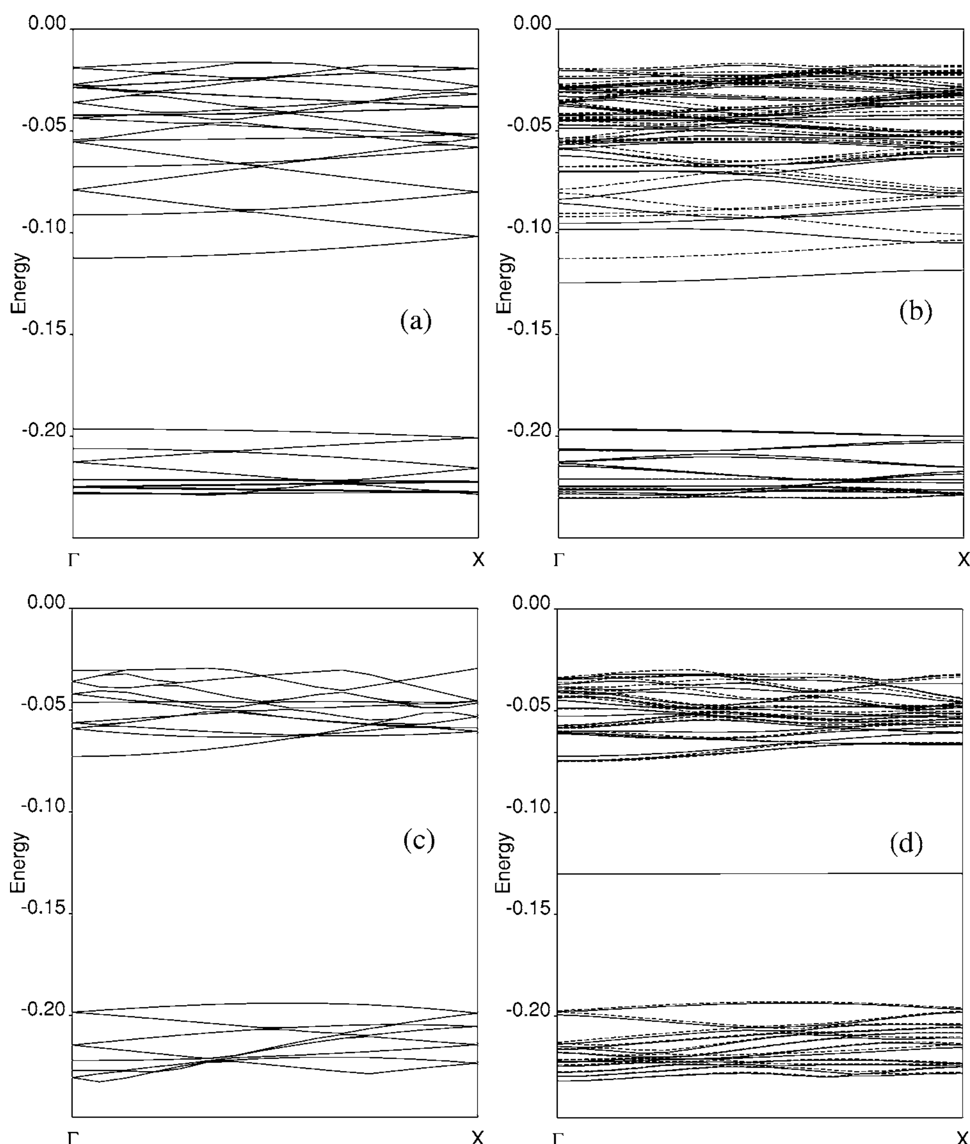

FIG. 2. The calculated BLYP band structure of the (a) perfect (8,0) SiC nanotube supercell, (b) nitrogen donor in the (8,0) SiC nanotube supercell, (c) perfect (6,6) SiC nanotube supercell, (d) nitrogen donor in the (6,6) SiC nanotube supercell close to the band gap. The straight and dotted lines represent the spin-up bands and spin-down bands in defective supercells, respectively. The spin-up donor level in the band gap is occupied by one electron. The energy scale is given in atomic units.

of the band gap. This convergence test shows that by using our parameters we do not achieve the absolute convergence but we are not far from that. In any case, the converged value of the LDA band gap should be even larger than 1.21 eV. Based on this convergence test the uncertainty here could be around 0.05 eV. In the supercell calculations with large number of basis functions the use of the parameters belonging to the absolute convergence would be too costly, therefore it seems to be a good compromise to use the parameters written in the methodology and to keep the uncertainty in the calculated LDA band gap in mind. It is well known that the LDA underestimates the width of the band gap due to the self-interaction of the electrons. The well-chosen BLYP functional calculation on this system resulted in 2.28 eV for the width of the band gap. This is about 1 eV higher than the LDA band gap similar to the earlier findings in bulk SiC polytypes.[30]

The structure of the optimized (6,6) SiC nanotubes shows similar properties as those of (8,0) nanotubes. The obtained Si-C bond length is about 1.78 Å in accordance with earlier studies.[6,9] We obtained a similar rippled surface as in the (8,0) SiC nanotube. The calculated average diameter is about 10.2 Å, while the optimized lattice constant is about 3.08 Å. The calculated band structure along Γ-*X* basically agrees with earlier works using similar methodology;[7,8] we obtained an indirect semiconductor, where the CBM is at the *X* point while the VBM is along Γ-*X* at about $0.64\pi/L$, where L is the lattice constant. The calculated indirect LDA and BLYP band gaps are 2.03 eV and 3.30 eV, respectively. Again, the BLYP band gap is about 1.3 eV larger than the LDA value. The BLYP band gap should be close to the experimental value.

The calculated LDA energy difference per Si-C unit between the two structures is about 0.09 eV favoring the (6,6)

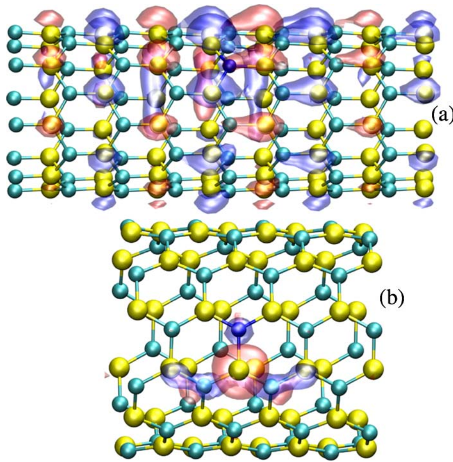

FIG. 3. (Color online) The calculated spatial distribution of the donor wave function of N_C is shown (a) in (8,0), (b) in (6,6) nanotubes. The red (blue) transparent lobes indicate the positive (negative) value of the wave function. Small (large) balls are the carbon (silicon) atoms, the nitrogen atom is the small dark blue ball.

nanotube with larger diameter. It is in accordance with the work of Miyamoto and Yu[5] (well-converged plane wave calculations) and with the work Zhao and co-workers[7] (using similar methodology). The calculated BLYP energy difference per Si-C unit is also about 0.09 eV. We have checked that the same physical properties obtained in the 128 atom and 96 atom supercells of (8,0) and (6,6) SiC nanotubes using 4 MP k points as in the appropriate primitive cells. We note here that the X point in the Brillouin zone (BZ) is projected into the Γ point of the reduced BZ of the supercell, therefore, the plotted band structure of the 96 atom (6,6) shows the CBM at the Γ point, i.e., at the projected X point. The calculated LDA energy difference per Si-C unit between the bulk 3C-SiC and the (6,6) SiC nanotube is about 1.59 eV favoring the bulk 3C-SiC as expected from earlier experimental[4] and theoretical studies,[6,7] so the SiC nanotubes are clearly metastable forms. The heat of formation of the nanotubes can be calculated as follows:

$$\Delta H_f = \mu_{\mathrm{SiC}}^{\mathrm{nanotube}} - (\mu_{\mathrm{Si}}^{\mathrm{bulk}} + \mu_{\mathrm{C}}^{\mathrm{bulk}}), \quad (2)$$

where $\mu_{\mathrm{SiC}}^{\mathrm{nanotube}}$ is the total energy per Si-C unit of the given SiC nanotube, i.e., the chemical potential of SiC nanotubes. The chemical potentials of silicon ($\mu_{\mathrm{Si}}^{\mathrm{bulk}}$) and carbon ($\mu_{\mathrm{C}}^{\mathrm{bulk}}$) are obtained from bulk Si and diamond. While the calculated heat of formation of these SiC nanotubes are positive [about 1.2 eV and 1.3 eV for (6,6) and (8,0) SiC nanotubes, respectively], the cohesion energy is far negative with respect to the energy of the isolated Si and C atoms. This can stabilize the metastable SiC nanotubes. A similar conclusion has been reached also in a theoretical work within a molecular cluster approach.[41]

B. Nitrogen substitutional in single wall SiC nanotubes

Nitrogen inclusively prefers the carbon site in bulk SiC.[10–12] The reason for this strong preference is due to the small relaxation energy at the carbon site (while large relaxation would be needed at the silicon site) on one hand, and the ionic character of nitrogen repels the electronegative C atoms in bulk SiC on the other hand. Since the situation is very similar in SiC nanotubes[7] only N_C is considered in this work. The optimized geometry is shown in both SiC nanotubes in Fig. 1. In the LDA calculation N_C is an effective mass like donor in (8,0) SiC nanotube; the unpaired electron goes to a delocalized state split from the conduction band edge. As expected, the relaxation is tiny for this defect. The atoms move less than 0.02 Å from their original lattice host sites. Mulliken analysis shows an extra charge on the nitrogen atom with a similar value as on the carbon atoms in the SiC nanotube. In the LDA calculations the unpaired electron goes to a delocalized state split from the conduction band edge in the (8,0) SiC nanotube. The LDA band gap of the (8,0) SiC nanotube is about 1.2 eV. Due to the LDA gap error it might happen hypothetically that a localized defect level is placed above the conduction band edge in the LDA calculations but the localized defect level would fall in the experimental band gap. This would result in a false description of the defect showing an effective mass like donor by LDA, however, it would be a localized donor in fact. BLYP calculation in the (8,0) SiC nanotube (with 2.28 eV band gap) shows clearly that N_C is indeed an effective mass like donor and no localized defect level appears in the gap. The occupied shallow donor level is at about 0.33 eV below the conduction band edge, i.e., at E_V+1.95 eV, where E_V is the valence band top. Its dispersion follows closely the dispersion of the conduction band belonging to the perfect nanotube [see Fig. 2(a)]. The effective mass donor states in this relatively small supercell are certainly overlocalized. The donor ionization energy can be a bit shallower than the calculated one for a truly isolated donor. Nevertheless, the nature of this defect is apparent from Fig. 2(a); similar to the bulk SiC N_C acts as a shallow effective mass like donor in the (8,0) SiC nanotube. The localization of the donor wave function on nitrogen is about 1% as inferred from the wave function coefficients. The spatial distribution of the wave function is shown in Fig. 3(a). It is apparent that the donor wave function is delocalized in the whole supercell.

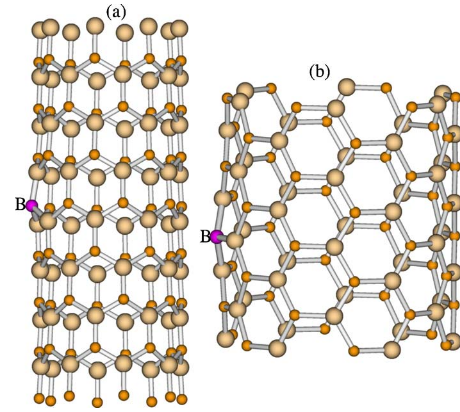

FIG. 4. (Color online) The optimized geometry of B_C in (a) (8,0), (b) (6,6) single wall SiC nanotubes. The large balls are the silicon atoms, the smaller balls are the carbon atoms. The boron atom is labeled.

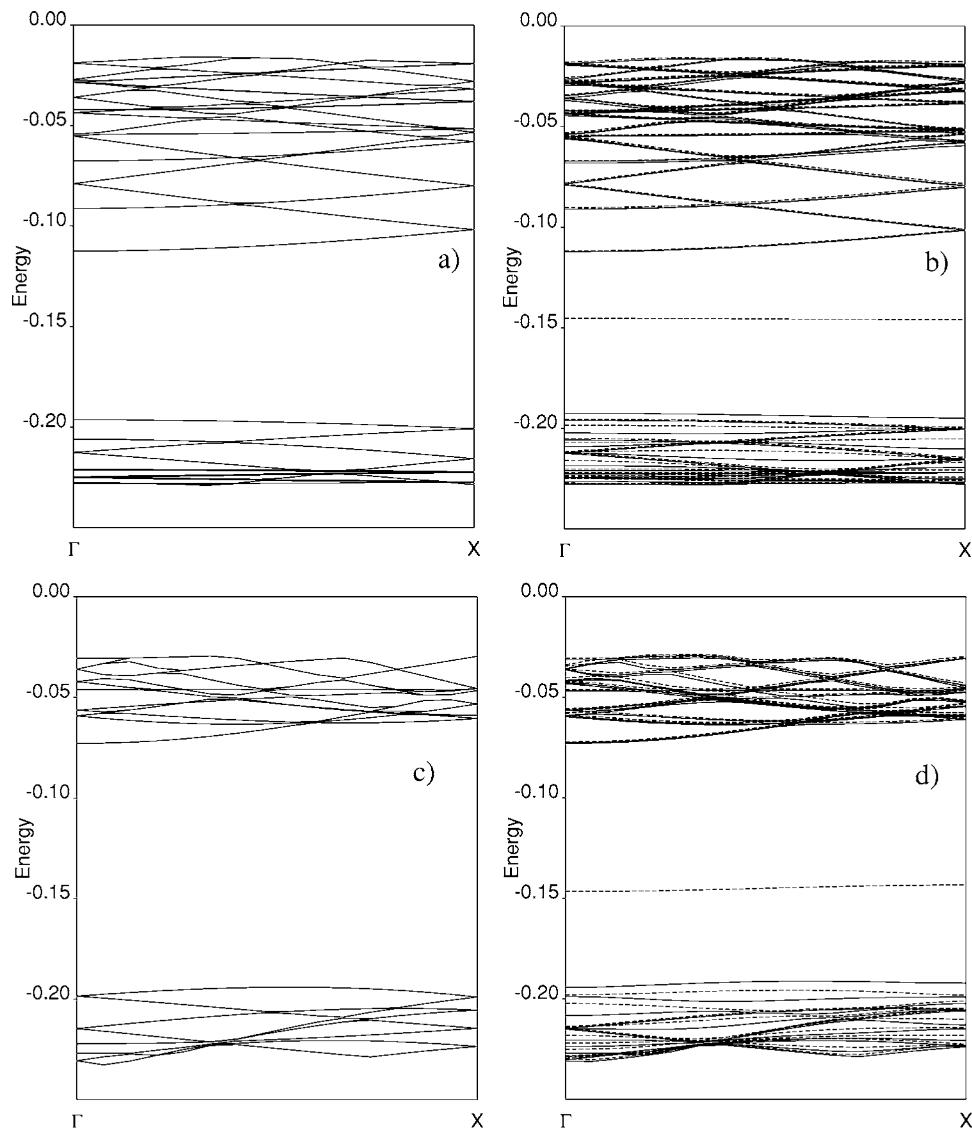

FIG. 5. The calculated BLYP band structure of the (a) perfect (8,0) SiC nanotube supercell, (b) B_C in (8,0) SiC nanotube supercell, (c) perfect (6,6) SiC nanotube supercell, (d) B_C in (6,6) SiC nanotube supercell close to the band gap. The straight and dotted lines represent the spin-up bands and spin-down bands in defective supercells, respectively. The highest spin-down defect level in the band gap is the empty acceptor level. The energy scale is given in atomic units.

In the (6,6) SiC nanotube the situation is different. The LDA band gap is about 2.0 eV. In the LDA calculations a localized donor level appears about 0.33 eV below the conduction band edge ($=E_V+1.67$ eV) that does not follow the dispersion of the conduction band edge at all; it is almost completely flat. Two short (1.75 Å) and one long (1.85 Å) bonds forms between N and its nearest Si neighbor atoms. The latter Si atom moves outward a bit from the original position. In BLYP calculation the donor level remains localized and is "shifted" only slightly compared to the LDA level; it is at about $E_V+1.73$ eV. The occupied deep donor level does not show dispersion clearly indicating its localized nature [see Fig. 2(b)]. The localization of the donor wave function on nitrogen reaches at least 10% as inferred from the wave function coefficients. Thus, N_C is a deep donor in the (6,6) SiC nanotube. The donor wave function is mainly localized on the first neighbor Si atom next to the N atom and on its close vicinity as shown in Fig. 3(b).

One might conclude that N_C behaves like an effective mass donor in SiC nanotubes possessing a "small" band gap (2.3 eV or lower) while it is a deep donor in a wide band gap SiC nanotube. An important note here that nitrogen is an amphoteric trap for the charge carriers in wide band gap SiC nanotubes unlike the case of bulk SiC where it behaves like a shallow donor.

C. Boron substitutional in single wall SiC nanotubes

First, we considered the boron at the carbon site. While the boron atom is on-center in bulk SiC,[13] we found that boron strongly reconstructs outward in both SiC nanotubes (see Fig. 4). The B-Si distances are about 1.9 Å. That is considerably longer than the original Si-C bond length of 1.78 Å. Mulliken analysis shows that boron is strongly nega-

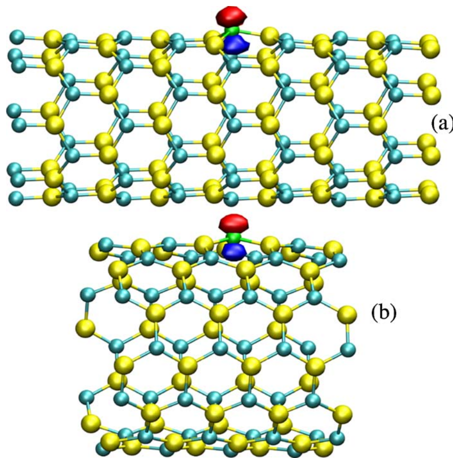

FIG. 6. (Color online) The calculated spatial distribution of the acceptor wave function of B_C is shown (a) in (8,0), (b) in (6,6) nanotubes. The red (blue) lobes indicate the positive (negative) value of the wave function. Small (large) balls are the carbon (silicon) atoms, the boron atom is the green ball.

tively ionized, stronger than carbon atoms in the host lattice. As the electronegative carbon atoms tend to relax outward the same happens to the boron atom. This effect is more pronounced than for carbon atoms since the electronegativity difference is even larger. B_C is an acceptor in both SiC nanotubes like in bulk SiC polytypes. The defect level of the unpaired electron in the LDA calculations is at about $E_V+0.18$ eV and $E_V+0.12$ eV in (8,0) and (6,6) SiC nanotubes, respectively. These states are valence band derived; the corresponding BLYP values are $E_V+0.10$ eV and $E_V+0.08$ eV, respectively (see Fig. 5). The valence band derived empty defect level falls relatively deeply into the band gap. The LDA-gap error should be very small in this case as it was shown for the occupied spin-up defect level. The empty acceptor level is at about $E_V+0.5$ eV in the LDA calculations which indicates that B_C is a relatively deep acceptor. The acceptor state is mostly localized on the p orbital of the boron atom pointing out along radial direction from the nanotube as shown in Fig. 6.

We studied the boron at the silicon site as well. Boron moves inward a bit from the lattice site. The obtained B-C distances are about 1.57 Å while the bond length between the second neighbor Si atoms and the nearest neighbor C atoms is elongated to about 1.80 Å (see Fig. 7). According to the Mulliken analysis the boron atom is slightly positively charged as expected from its position. B_{Si} is a shallow acceptor in both SiC nanotubes like in bulk SiC polytypes. The defect level of the unpaired electron in the LDA calculations is at about $E_V+0.08$ eV in both (8,0) and (6,6) SiC nanotubes. These states are valence band derived; the corresponding BLYP value is $E_V+0.10$ eV in both SiC nanotubes (see Fig. 8). The valence band derived empty defect level is also close to the band gap. The LDA gap error should be very small in this case as it was shown for the occupied spin-up defect level. The empty acceptor level is at about $E_V+0.17$ eV in the LDA calculations which indicates that B_{Si} is a shallow acceptor. Indeed, the acceptor state of B_{Si} is more spread out than that of B_C as shown in Fig. 9. The acceptor

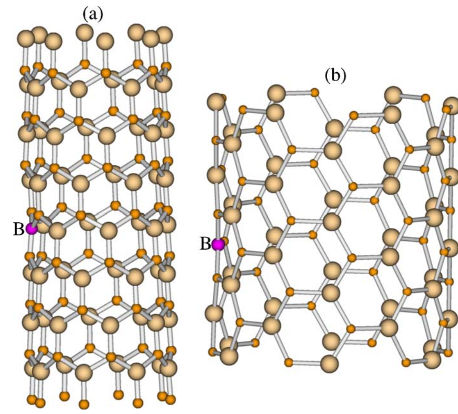

FIG. 7. (Color online) The optimized geometry of B_{Si} in (a) (8,0), (b) (6,6) single wall SiC nanotubes. The large balls are the silicon atoms, the smaller balls are the carbon atoms. The boron atom is labeled.

state is mainly localized on the p orbitals of the two near carbon neighbor atoms of the boron atom in the (8,0) SiC nanotube while it is localized mostly on the p orbital of one near carbon atom and less on that of the other two near carbon atoms in the (6,6) SiC nanotube. The acceptor state is not localized at all on the boron atom in this case unlike in B_C defect. Finally, we summarize the calculated vertical ionization energies for the defects under consideration in Table I.

While both B_C and B_{Si} form acceptor states in SiC nanotubes, it is of interest to study which one is favored. Following the equations of Northrup and co-workers[42] one can calculate the formation energy of defects. In compound semiconductors the chemical potential of the host constituents depends on the stoichiometry of the material; the theoretical limits are $\mu_{Si}=\mu_{Si}^{bulk}$ and $\mu_C=\mu_C^{bulk}$ which correspond to extreme Si-rich and C-rich conditions, where μ_{Si}^{bulk} and μ_C^{bulk} are defined as in Eq. (2). As an example, one can calculate the energy difference (ΔE) of the formation energies of B_{Si} between at extreme Si-rich and C-rich conditions, respectively,

$$\Delta E = E_{form}^{Si\text{-}rich}(B_{Si}) - E_{form}^{C\text{-}rich}(B_{Si}) = \mu_{Si}^{bulk} + \mu_C^{bulk} - \mu_{SiC}^{nanotube} = -\Delta H_f. \quad (3)$$

In bulk SiC the heat of formation (ΔH_f) is negative, therefore, ΔE is positive. This means that the formation of B_{Si} is favorable under the C-rich condition with respect to the Si-rich condition in bulk SiC. However, SiC nanotubes are metastable solids and, in fact, the calculated ΔH_f of SiC nanotubes is positive. This means that the formation of B_{Si} will be favorable under the Si-rich condition with respect to the C-rich condition in SiC nanotubes unlike in bulk SiC polytypes. We have to add that $\mu_{Si}=\mu_{Si}^{bulk}$ and $\mu_C=\mu_C^{bulk}$ are only theoretical limits. A theoretical study predicts[41] that SiC nanotubes are stable up to 1:1 ratio of Si:C and they dissociate at a higher ratio while they are stable at a lower ratio. This indicates that the range only between stoichiometry (at 1:1 of Si:C ratio) and the C-rich condition must be taken into

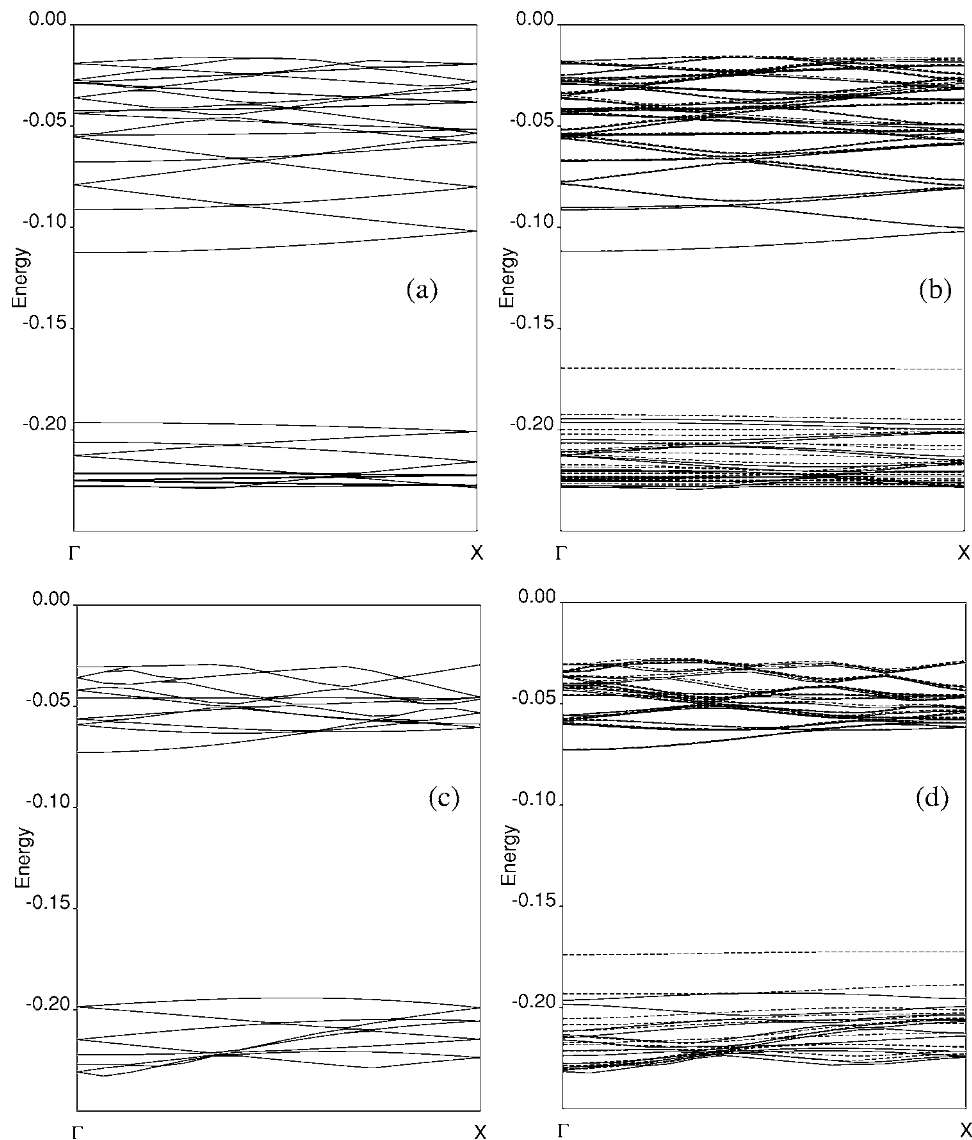

FIG. 8. The calculated BLYP band structure of the (a) perfect (8,0) SiC nanotube supercell, (b) B_{Si} in the (8,0) SiC nanotube supercell, (c) perfect (6,6) SiC nanotube supercell, (d) B_{Si} in the (6,6) SiC nanotube supercell close to the band gap. The straight and dotted lines represent the spin-up bands and spin-down bands in defective supercells, respectively. The highest spin-down defect level in the band gap is the empty acceptor level. The energy scale is given in atomic units.

account. The difference in the formation energies of B_{Si} and B_C $[\Delta E(B)]$ is

$$\Delta E(\mathrm{B}) = \Delta E_{\mathrm{tot}}(\mathrm{B}) + \mu_{\mathrm{SiC}}^{\mathrm{nanotube}} - 2\mu_{\mathrm{C}} \quad (4)$$

where $\Delta E_{tot}(B)$ is the total energy difference of B_{Si} and B_C in the appropriate supercells. In stoichiometry $(\mu_C = \mu_C^{bulk} - \Delta H_f/2)$ Eq. (4) yields about −0.4 eV while in the C-rich condition it is about 0.9 eV in the (8,0) SiC nanotube.[43] In other words, close to stoichiometry both B_{Si} and B_C form (B_{Si} in greater extent) while in the C-rich condition B_C preferentially forms. We have to add that the presence of hydrogen might change the site preference of boron like in bulk SiC polytypes.[44] Work is in progress in this direction.

IV. SUMMARY

The structure and electronic properties of substitutional nitrogen and boron impurities have been studied in single wall SiC nanotubes. It was found that nitrogen forms a shallow donor state or it is a charge carrier trap depending on the width of the band gap of SiC nanotubes while boron can form shallow and relatively deep acceptor states depending on the stoichiometry of SiC nanotubes. The nitrogen cannot act as an *n*-type dopant in wide band gap SiC nanotubes unlike the case of bulk SiC, it is rather a compensating center both for the holes and for the electrons. Nevertheless, the nitrogen can be used in the small band gap (<2.3 eV) SiC nanotubes as an *n*-type dopant. The calculated ionization energy is about 0.3 eV which is deeper by about 0.15–0.2 eV than in bulk SiC polytypes. Still, in high temperature applications it can be a suitable *n*-type dopant. Boron behaves

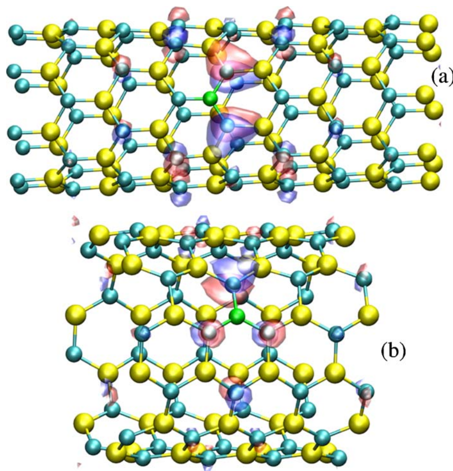

FIG. 9. (Color online) The calculated spatial distribution of the acceptor wave function of B_{Si} is shown (a) in (8,0), (b) in (6,6) nanotubes. The transparent red (blue) lobes indicate the positive (negative) value of the wave function. Small (large) balls are the carbon (silicon) atoms, and the boron atom is the green ball.

similarly in SiC nanotubes like in bulk SiC. B_{Si} is a relatively shallow acceptor while B_C is a relatively deep acceptor with similar levels like in bulk SiC. B_{Si} is a common *p*-type dopant in bulk SiC, thus it would be a *p*-type dopant in SiC nanotubes as well. If the concentration of nitrogen can be controlled then the Fermi level of SiC nanotubes can be manipulated: in small band gap SiC nanotubes it acts as *n*-type donor pushing the Fermi level up in the band gap while in wide band gap SiC nanotubes it can pin the Fermi level close to the midgap, making those to be semi-insulating. If the concentration *and* the site selection of boron can be controlled, then the Fermi level can be close to the valence band top. The manipulation of the Fermi level in SiC nanotubes can be an important issue in biological applications and in chemical sensors.

TABLE I. The calculated vertical ionization energies of the nitrogen donor and boron acceptors in (8,0) and (6,6) SiC nanotubes. The ionization energies are given with respect to the conduction band edge for the nitrogen donor and to the valence band edge for boron acceptors, respectively. The estimated uncertainty in the calculations is about 0.05 eV according to the convergence test (see text). The units are in eV.

	(8,0)	(6,6)
N_C	0.3	1.6
B_C	0.5	0.5
B_{Si}	0.2	0.2

[1] S. Iijima, Nature (London) **354**, 56 (1991).
[2] A. P. Alivisatos, Science **271**, 933 (1996).
[3] E. W. Wong, P. E. Sheehan, and C. M. Lieber, Science **277**, 1971 (1997).
[4] X.-H. Sun, C.-P. Li, W.-K. Wong, N.-B. Wong, C.-S. Lee, and B.-K. Teo, J. Am. Chem. Soc. **124**, 14464 (2002).
[5] Y. Miyamoto and B. D. Yu, Appl. Phys. Lett. **80**, 586 (2002).
[6] M. Menon, E. Richter, A. Mavrandonakis, G. Froudakis, and A. N. Andriotis, Phys. Rev. B **69**, 115322 (2004).
[7] M. Zhao, Y. Xia, F. Li, R. Q. Zhang, and S.-T. Lee, Phys. Rev. B **71**, 085312 (2005).
[8] M. Zhao, Y. Xia, R. Q. Zhang, and S.-T. Lee, J. Chem. Phys. **122**, 214707 (2005).
[9] F. Li, Y.-Y. Xia, M.-W. Zhao, X.-D. Liu, B.-D. Huang, Z.-H. Yang, Y.-J. Ji, and C. Song, J. Appl. Phys. **97**, 104311 (2005).
[10] A. Gali, P. Deák, N. T. Son, and E. Janzén, Appl. Phys. Lett. **83**, 1385 (2003).
[11] R. Rurali, P. Godignon, J. Rebollo, E. Hernández, and P. Ordejón, Appl. Phys. Lett. **82**, 4298 (2003).
[12] M. Bockstedte, A. Mattausch, and O. Pankaratov, Appl. Phys. Lett. **85**, 58 (2004).
[13] A. Fukumoto, Phys. Rev. B **53**, 4458 (1996).
[14] M. Bockstedte, A. Mattausch, and O. Pankratov, Phys. Rev. B **70**, 115203 (2004).
[15] A. Gali, T. Hornos, P. Deák, N. T. Son, E. Janzén, and W. J. Choyke, Appl. Phys. Lett. **86**, 102108 (2005).
[16] M. Bockstedte, A. Mattausch, and O. Pankratov, Mater. Sci. Forum **353-356**, 447 (2001).
[17] P. Deák, B. Aradi, A. Gali, U. Gerstmann, and W. J. Choyke, Mater. Sci. Forum **433-436**, 523 (2003).
[18] S. Greulich-Weber, Phys. Status Solidi A **162**, 95 (1997).
[19] H. Itoh, T. Troffer, C. Peppermüller, and G. Pensl, Appl. Phys. Lett. **73**, 1427 (1998).
[20] W. Suttrop, G. Pensl, and P. Lanig, Appl. Phys. A **51**, 231 (1990).
[21] Y. Gao, S. I. Soloviev, and T. S. Sudarshan, Appl. Phys. Lett. **83**, 905 (2003).
[22] S. G. Müller, M. F. Brady, W. H. Brixius, R. C. Glass, H. M. Hobgood, J. R. Jenny, R. T. Leonard, D. P. Malta, A. R. Powell, V. F. Tsvetkov, S. T. Allen, J. W. Palmour, and C. H. Carter, Jr., Mater. Sci. Forum **433-436**, 39 (2003).
[23] A. Ellison, B. Magnusson, N. T. Son, L. Storasta, and E. Janzén, Mater. Sci. Forum **433-436**, 33 (2003).
[24] M. A. Lienhard and D. J. Larkin, http://www.grc.nasa.gov/WWW/RT2002/5000/5510lienhard.html
[25] W. Kohn and L. J. Sham, Phys. Rev. Lett. **140**, A1133 (1965).
[26] J. M. Soler, J. D. Gale, A. García, J. Junquera, P. Ordejón, and D. Sanchéz-Portal, J. Phys.: Condens. Matter **14**, 2745 (2002).
[27] D. M. Ceperley and B. J. Alder, Phys. Rev. Lett. **45**, 566 (1980).
[28] J. P. Perdew and A. Zunger, Phys. Rev. B **23**, 5048 (1981).
[29] N. Troullier and J. L. Martins, Phys. Rev. B **43**, 1993 (1991).
[30] A. Gali, P. Deák, P. Ordejón, N. T. Son, E. Janzén, and W. J. Choyke, Phys. Rev. B **68**, 125201 (2003).
[31] H. J. Monkhorst and J. K. Pack, Phys. Rev. B **13**, 5188 (1976).
[32] J. Muscat, A. Wander, and N. Harrison, Chem. Phys. Lett. **34**, 397 (2001).
[33] J. Heyd and G. Scuseria, J. Chem. Phys. **121**, 1187 (2004).
[34] In the CRYSTAL2003 code it is possible to use periodic boundary condition only in one dimension, so the spurious tube-tube interactions certainly do not arise here.

[35] A. Becke, J. Chem. Phys. **98**, 5648 (1996).
[36] V. R. Saunders, R. Dovesi, C. Roetti, M. Causá, N. M. Harrison, R. Orlando, and C. M. Zicovich-Wilson, *CRYSTAL2003 User's Manual* (University of Torino, Torino, 2003).
[37] J. C. Barthelat and P. Durand, Mol. Phys. **159**, 1187 (1977).
[38] M. Causá, R. Dovesi, and C. Roetti, Phys. Rev. B **43**, 11937 (1991).
[39] J. Furthmüller, G. V. Cappellini, H.-C. Weisser, and F. Bechstedt, Phys. Rev. B **66**, 045110 (2002).
[40] M. Menon and D. Srivastava, Chem. Phys. Lett. **307**, 407 (1999).
[41] A. Mavrandonakis, G. E. Froudakis, M. Schnell, and M. Mühlhäuser, Nano Lett. **3**, 1481 (2003).
[42] J. E. Northrup, R. Di Felice, and J. Neugebauer, Phys. Rev. B **56**, R4325 (1997).
[43] The LDA values and BLYP values are the same within the expected accuracy (0.05 eV).
[44] B. Aradi, P. Deák, N. T. Son, E. Janzén, W. J. Choyke, and R. P. Devaty, Appl. Phys. Lett. **79**, 2746 (2001).